EPJ E
Soft Matter and Biological Physics
EPJ.org
your physics journal

Eur. Phys. J. E **29**, 123–130 (2009) DOI: 10.1140/epje/i2009-10457-y

# Transmission of ultrasound through a single layer of bubbles

V. Leroy, A. Strybulevych, M.G. Scanlon and J.H. Page

EDP SCIENCES
Società Italiana di Fisica
Springer

Eur. Phys. J. E **29**, 123–130 (2009)
DOI 10.1140/epje/i2009-10457-y

THE EUROPEAN PHYSICAL JOURNAL E

Regular Article

# Transmission of ultrasound through a single layer of bubbles

V. Leroy[1,a], A. Strybulevych[1], M.G. Scanlon[2], and J.H. Page[1,b]

[1] Department of Physics and Astronomy, University of Manitoba, Winnipeg, Canada
[2] Department of Food Science, University of Manitoba, Winnipeg, Canada

Received 22 August 2008 and Received in final form 1 April 2009
Published online: 13 May 2009 – 

**Abstract.** We investigate, both experimentally and theoretically, the effect of coupling between resonant scatterers on the transmission coefficient of a model system of isotropic scatterers. The model system consists of a monodisperse layer of bubbles, which exhibit a strong monopole scattering resonance at low ultrasonic frequencies. The layer was a true 2D structure obtained by injecting very monodisperse bubbles (with radius $a \sim 100\,\mu$m) into a yield-stress polymer gel. Even for a layer with a low concentration of bubbles (areal fraction, $n\pi a^2$, of 10–20%, where $n$ is the number of bubbles per unit area), the ultrasonic transmission was found to be significantly reduced by the presence of bubbles ($-20$ to $-50$ dB) and showed a sharp minimum at a particular frequency. Interestingly, this frequency did not correspond to the resonance frequency of the individual, isolated bubbles, but depended markedly on the concentration. This frequency shift is an indication of strong coupling between the bubbles. We propose a simple model, based on a self-consistent relation, which takes into account the coupling between the bubbles and gives good agreement with the measured transmission coefficient.

**PACS.** 43.35.+d Ultrasonics, quantum acoustics, and physical effects of sound – 43.20.+g General linear acoustics

## 1 Introduction

During the last decade, there has been increasing interest in the wave physics of complex materials, particularly in the context of exotic phenomena such as Anderson localization in strongly disordered media [1,2] or negative refraction in novel metamaterials [3]. In both cases, resonances can play a vital role, either to ensure strong scattering which is a necessary condition for localization or to manipulate the phase so as to create unusual wave propagation effects. For metamaterials, low-frequency resonances, for which the wavelength is much larger than the scattering unit, are crucial [3]. For materials with acoustic resonances, bubbles are especially interesting, as they are strong acoustic scatterers that exhibit a low-frequency resonance known as the Minnaert resonance [4]. As a consequence, propagation of acoustic waves is drastically affected by the presence of bubbles in a liquid and this problem has been the subject of extensive studies [5–17]. Indeed, bubbly media may be considered as acoustic metamaterials, as they exhibit exotic properties such as a very small phase velocity at low frequencies and a bandgap associated with resonances, regardless of whether the bubbles are ordered or not. In view of these rather spectacular properties, and the inherent simplicity of a bubble's monopole resonance, bubbly media are often regarded as model systems for acoustic studies, which have the potential to address fundamental questions that may be relevant for the transport of any type of wave through materials where strong wave scattering plays an important role.

One of the key issues for wave transport in strongly scattering materials is the effect of coupling between scatterers near resonance, an effect that makes the traditional independent scatterers approximation (ISA) inadequate. To correctly account for the scattering from any scatterer when the concentration becomes large, the influence of the other scatterers must be included —a process called dependent or recurrent scattering. In many previous studies of wave propagation in strongly scattering media, interest in the breakdown of the ISA has focused on interference effects associated with the approach to Anderson localization. Another possible effect of dependent scattering is a shift in the resonance frequency of the scatterers. This effect can be treated theoretically via effective medium models [18], but since the effect is often rather small, it can be difficult to detect, and so is frequently overlooked. To gain a better understanding of the underlying physics, a combination of experiment and theory on a system exhibiting a large resonant frequency shift is needed. Acoustic resonances in a well-controlled bubbly dispersion may

[a] *Present address:* Laboratoire Matière et Systèmes Complexes, Université Paris Diderot-Paris 7, CNRS (UMR 7057), 10 rue Alice Domon et Léonie Duquet, 75205 Paris, France; e-mail: `valentin.leroy@univ-paris-diderot.fr`
[b] e-mail: `jhpage@cc.umanitoba.ca`

be good candidates to address this manifestation of the breakdown of the ISA.

While different corrections to the ISA have been proposed for bubbly media, no clear consensus exists about which one is correct [13–16,19–22] and experimental data are lacking. Indeed, on the one hand, experiments with a finite number of bubbles are relatively numerous and clearly demonstrate that the coupling between bubbles plays an important role [23–26]. On the other hand, experiments with a *continuum* of bubbles are often limited to frequencies below or above the resonance [27–30] and seldom investigate the resonance [5,7,31]. This lack of data can be explained by the huge attenuation of sound in bubbly media around the resonance frequency, which makes precise measurements a difficult task. Consequently, how the coupling between bubbles should be taken into account to correct the ISA formulation is still an open question.

An alternative approach to the ISA and its possible corrections is the Multiple Scattering Theory (MST) [6, 32–34], which provides a systematic and accurate way to take into account the coupling between the scatterers. However, its exact implementation is limited to perfectly *ordered* systems, or to a finite number of *disordered* scatterers. This limitation to a finite number of scatterers in the disordered case is particularly critical when the scatterers are bubbles. Since the frequencies of interest correspond to large wavelengths compared to the typical distance between bubbles, a large number of scatterers is required in the finite system to give information that is relevant to macroscopic samples.

In this paper, we investigate the effect of dependent scattering on the resonant frequency of an ensemble of bubbles by reporting measurements of the acoustic transmission through *one* layer of identical bubbles. A layer of bubbles presents the double advantage of being thin, so that the transmission of sound remains measurable, and of being a geometry simple enough to make analytical calculations possible. Note that we use the term layer to refer to an assembly of bubbles located on the same plane, *i.e.* a 2D structure. This case differs from the thin layer of bubbles sometimes investigated in the literature [11,35] which refers to a thin 3D structure. To our knowledge, the problem of the acoustic properties of one plane of bubbles has never been studied experimentally. We interpret our experimental observations by developing a theoretical model that accounts for the interaction between bubbles, thereby extending previous calculations for a plane of isotropic scatterers [36,37] and giving a simple physical picture of the origin of the resonance shift. We find that the large shifts in the resonant frequency that we measure experimentally at low concentrations of bubbles are well explained by our model.

## 2 Experimental set-up

### 2.1 Sample preparation

The production of 2D samples of identical bubbles was obtained with a home-made set-up [31], whose key innovation was the use of a yield-stress polymer fluid as a matrix for the injection of the bubbles. We used a commercial hair gel (Dep, sport endurance gel, made in USA by Henkel corporation) diluted with water and degassed. The benefit of the hair gel for this experiment is that it flows only if the applied stress is larger than a threshold value (the yield stress). Hence if bubbles are sufficiently small, they remain trapped in the gel at the exact place where they have been injected.

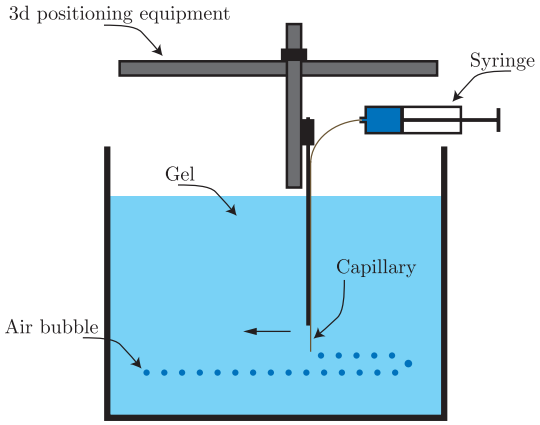


**Fig. 1.** Injection of bubbles: a capillary is moved in a pre-programmed pattern of positions within the gel, delivering rows of equally sized bubbles. The speed $V$ at which the capillary was moved and the pressure $P$ in the syringe are the two parameters governing the bubble size and the distance between bubbles.

The injection was performed as depicted in Figure 1. A thin capillary (inner diameter of $20\,\mu$m), connected to a syringe with air at pressure $P$, was moved at constant speed $V$ in the gel. With a well-controlled flow of gas through the capillary, as set by the pressure $P$, the movement generated an array of equally spaced bubbles of the same size. Thanks to a 3D displacement stage, the vertical distance between successive rows of bubbles could be pre-programmed, depending on the desired total concentration.

Although a discussion of the exact mechanisms involved in this process is outside the scope of this article, we note that by varying the two parameters $P$ and $V$, different bubble radii $a$ and distances between bubbles $d$ could be obtained. Examples of injections with different speeds and pressures are given in Figure 2. Typically, small bubbles separated by large distances were obtained with low pressures and high speeds ($a = 80\,\mu$m and $d = 1060\,\mu$m for $P = 1.33\,$bar and $V = 1\,$cm/s), whereas high pressures and low speeds generated big bubbles almost in contact ($a = 170\,\mu$m and $d = 355\,\mu$m for $P = 2\,$bar and $V = 0.2\,$cm/s). All the configurations between those two extreme cases were possible by a fine tuning of $P$ and $V$. Therefore, the device made possible the injection of quasi-ordered monodisperse layers of bubbles, with a good control of the size and the concentration. However, the bubbles were never arranged in a perfect crystal, because it was impossible to achieve a good "synchronization" from one line to the other. As a result, there was an offset in

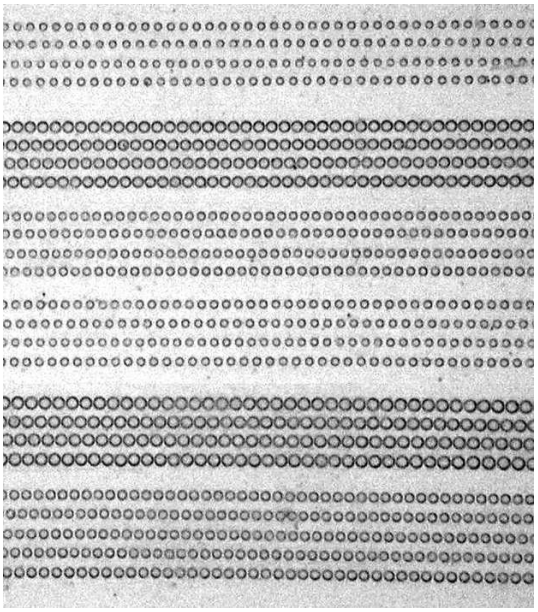

**Fig. 2.** Examples of bubble arrays obtained with the injection apparatus shown in Figure 1, under six different conditions. The three top series of four lines were injected with $P = 1.8\,\text{bar}$, and $V = 1$, 0.2, 0.5 cm/s from top to bottom. The three bottom series of lines were injected with $P = 2\,\text{bar}$, and the same sequence of speeds.

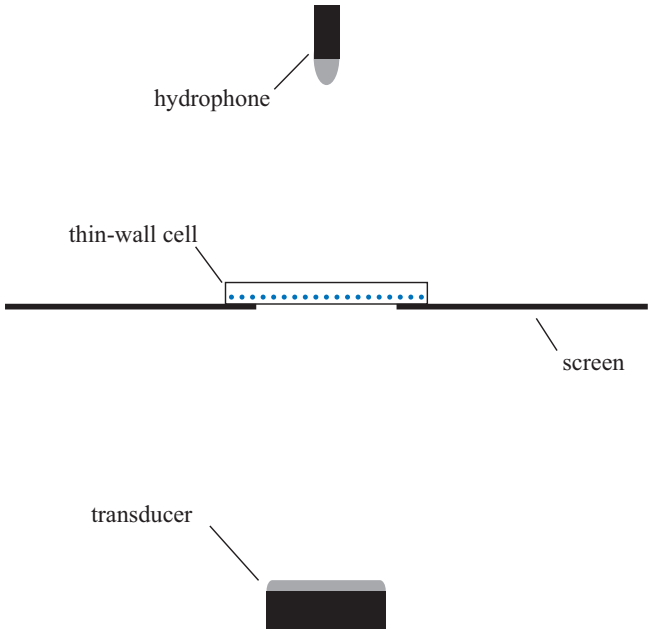


**Fig. 3.** Sketch of the set-up for ultrasonic measurements. A piezoelectric transducer emits an acoustic pulse that traverses the cell containing the layer of bubbles and is detected by a hydrophone.

the position of the bubbles, as is apparent in Figure 2, for instance. The edges of the bubble array were even more imperfect: since the motor stage needed to decelerate before turning to the next line, bubbles on the edges tended to be significantly bigger that the ones in the middle of the sample.

An important issue was the stability of the sample: if the degassed gel was undersaturated with air, bubbles dissolved in a matter of minutes. To prevent this, an interval of several days was required between the degassing of the gel and the injection, so that the gel was saturated. With this precaution, samples were stable over several hours, and it was checked that the size of the bubbles was not changing during the course of the ultrasonic measurements.

## 2.2 Ultrasonic measurements

Samples were injected with bubbles in a 1.2 cm thick cell that was filled with the gel. The walls of the cell were made from a very thin sheet of plastic (0.1 mm). From the acoustic point of view, the gel was very similar to water and the walls were transparent, at least for the frequencies considered in these experiments ($\sim 100\,\text{kHz}$). Thus, when no bubbles were present, we can consider the cell to be equivalent to a slab of water. This equivalence was checked experimentally by measuring both the longitudinal and shear moduli of the gel. The longitudinal modulus, as determined from the longitudinal ultrasonic velocity $v$, was found to be identical to water ($\beta' = 2.3\,\text{GPa}$, with $\beta''$ too small to measure at these frequencies). The complex shear modulus of the gel was also measured, using standard rheological techniques, at frequencies up to 100 Hz: the results are $\mu' = 60\,\text{Pa} \times (\frac{\omega}{2\pi\,\text{Hz}})^{0.1}$ and $\mu'' = 13\,\text{Pa} \times (\frac{\omega}{2\pi\,\text{Hz}})^{0.5}$. Thus, by any plausible extrapolation of the shear modulus data to ultrasonic frequencies, the shear modulus is so much smaller than the longitudinal modulus that its effects on the acoustic properties of the gel are likely to be negligible. The shear modulus is also much smaller than the longitudinal modulus of the air ($\beta'_{\text{air}} = 0.14\,\text{MPa}$) and thus does not affect the dynamics of the bubbles. This was checked by measuring the resonance frequency of single bubbles of different radii in the gel, using the same method as in reference [38]. These measurements showed that the Minnaert formula, derived for bubbles in a liquid, is also valid in the gel.

The acoustic properties of the samples were measured with the set-up of Figure 3. In a large tank ($60 \times 60 \times 120\,\text{cm}^3$) filled with reverse osmosis water, a piezoelectric transducer generated a pulse that propagated through water, traversed the sample and reached the hydrophone. The amplitude of the acoustic signal was small enough ($\sim 10^3\,\text{Pa}$) to prevent non-linear response of the bubbles. Because the transmission through the layer of bubbles was low, and because the divergence of the beam was not negligible (especially at low frequencies), the use of a screen (a plastic ring wrapped with Teflon tape) was essential for reducing spurious signals. The aperture, $D$, of the screen was larger than the wavelength of the pulse to limit diffraction effects, but smaller than the typical size on which the layer of bubbles could be considered to be uniform (*i.e.* the bad edges of the injected area were excluded from the measurement). In our experiments, $D$ was 6 cm, the lines

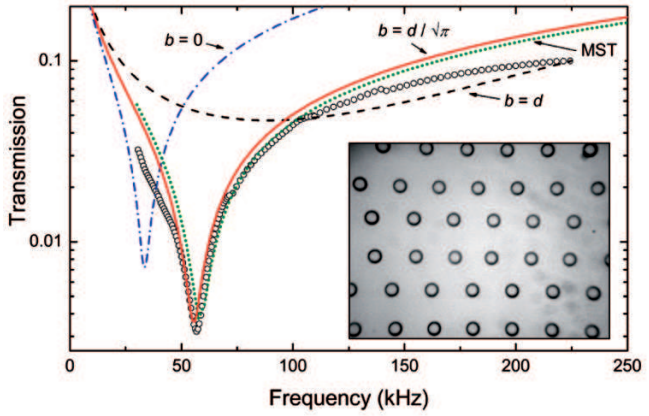


**Fig. 4.** Magnitude of the amplitude transmission coefficient through one layer of 94 $\mu$m radius bubbles separated on average by 530 $\mu$m (see inset) as a function of frequency. Open circles: experimental data. Solid, dashed and dash-dotted lines: model with three possible cutoffs, $b = d/\sqrt{\pi}$, $b = d$ and $b = 0$, respectively (see text). Dotted line: MST prediction.

of bubbles were 8 cm long, and the maximum wavelength was 5 cm (for the lowest frequency of 30 kHz).

Gaussian pulses, with central frequencies ranging from 30 to 250 kHz, were generated by an arbitrary waveform generator connected to a piezoelectric transducer. The pulses were recorded, with a hydrophone, in two different cases: when the cell was mounted on the screen, and when the cell was absent. The signals were averaged over 100 acquisitions when the attenuation was low (for reference measurements, for example), and up to 5000 acquisitions for highly attenuated signals. The transmission coefficient through the layer of bubbles, $T$, was obtained by calculating the ratio of the Fourier transforms of the signals with and without the cell in the path of the acoustic beam. Such a method, *a priori*, gives the contribution to the transmission not only of the bubbles but also of the gel and the walls of the cell. However, it was verified that the cell filled with a bubble-free gel has a transmission coefficient of 1, justifying the suitability of our methodology for measuring the contribution of the bubbles only.

## 3 Results and discussion

Figure 4 shows the magnitude of the transmission measured through one layer of 94 $\mu$m radius bubbles separated by 530 $\mu$m. The first observation is that even a small fraction of bubbles (here the areal fraction is 10%) can efficiently block the propagation of low frequency ultrasound. The presence of the layer reduces the amplitude of the sound by more than a factor 10 throughout the 100–250 kHz frequency band. The transmission can even be much lower and reaches a minimum of $3 \times 10^{-3}$ at 56 kHz. Interestingly, this frequency is 70% higher than the resonance frequency of the individual bubbles of the layer ($\sim$ 33 kHz). This is a clear evidence of the strong coupling between bubbles. Note that the shift of the resonance frequency to a *higher* frequency may seem surprising. Indeed, as the bubbles of the plane are driven in phase by the incoming plane wave, we could expect a *lowering* of the resonance frequency, as usually observed for a system of oscillators in phase.

A *single* isotropic scatterer excited by an incoming monochromatic plane wave $p_e \exp(ikx - i\omega t)$ generates a spherical field $(fp_e/r)\exp(ikr - i\omega t)$, where $f$ is the scattering function of the scatterer. For a bubble of radius $a$, $f$ is given by

$$f = \frac{a}{\left(\frac{\omega_0}{\omega}\right)^2 - 1 - i\delta}, \tag{1}$$

where $\omega_0$ is the Minnaert resonance of the bubble and $\delta$ its damping constant [4,39,40]. The bubbles' oscillations are damped by three mechanisms: viscosity, thermal losses and radiation. For the sake of simplicity, we will focus for now on the radiative damping and take $\delta = ka$; in the comparison of theory with experiment later on, we include all contributions to $\delta$. Note that all our results in this article are valid for frequencies low enough to ensure that $ka \ll 1$ (*i.e.* the bubble's radius is much smaller than the wavelength). For bubbles, this condition is not at all restrictive because the Minnaert resonance is a very low frequency resonance: $\omega_0 a/v \sim 10^{-2}$.

A *plane* of isotropic scatterers excited by a monochromatic plane wave $p_e \exp(ikx - i\omega t)$ generates a plane wave with amplitude $2i\pi f n p_e/k$ [41], where $n$ is the number of scatterers per unit area. Thus the layer of scatterers gives rise to a transmitted plane wave $Tp_e \exp(ikx - i\omega t)$ and a reflected plane wave $Rp_e \exp(-ikx - i\omega t)$ with

$$T = 1 + Kf, \tag{2}$$

$$R = Kf, \tag{3}$$

where $K = 2i\pi n/k$. Richard Feynman used these relations in his famous lectures [42] to introduce the physical principle of the optical index of a medium. If we consider that the plane of scatterers is a thin layer of homogeneous material with a thickness given by $d = 1/\sqrt{n}$, the phase difference induced by traversing the layer can be attributed to an effective wave number $\kappa = k + 2\pi f/(kd^3)$, which is nothing else but the expansion of the classical Foldy law: $\kappa^2 = k^2 + 4\pi N f$ [43], where $N$ is the number of scatterers per unit volume.

The previous calculation assumed that the scatterers were independent. In our case, we know that the presence of other bubbles around one bubble drastically modifies its scattering properties. Bubbles are usually strongly coupled to each other and the scattering function $f$ should be replaced with a new function $F$ accounting for the interactions between the bubbles: $Fp_e = fp_{tot}$, where $p_{tot}$ is the total field at each scatterer. In the general case, calculating $F$ is a difficult task [13,15]. But for the simple geometry of the plane, a considerable simplification occurs: all the bubbles are experiencing the same average field. Therefore we can consider, without loss of generality, the bubble located at the origin of our system of coordinates, which experiences a total pressure $p_{tot} = p_e(1 + \tilde{K}F)$, where $\tilde{K}$ is defined by

$$\tilde{K} = \sum_n \frac{1}{r_n} e^{ikr_n}, \tag{4}$$

the summation being over all the *other* bubbles of the plane and $r_n$ denoting the distance of bubble $n$. By the definitions of $F$ and $f$, one then obtains the self-consistent relation $F = f(1 + \tilde{K}F)$ which leads to

$$F = \frac{f}{1 - \tilde{K}f} \tag{5a}$$

$$= \frac{a}{\left(\frac{\omega_0}{\omega}\right)^2 - 1 - \mathrm{i}\delta - \tilde{K}a}\,. \tag{5b}$$

The last step to obtain a complete expression for the transmission through a plane of bubbles is the evaluation of $\tilde{K}$. The approximation of a continuous distribution of scatterers on the plane allows us to use an integral expression

$$\tilde{K} \simeq \int_b^\infty 2\pi n \mathrm{e}^{\mathrm{i}kr}\mathrm{d}r = K\mathrm{e}^{\mathrm{i}kb}, \tag{6}$$

where $b$ is a cutoff distance below which no other bubbles are supposed to be found. With this notation the transmission coefficient $T = 1 + KF$ becomes

$$T = 1 + \frac{Kf}{1 - Kf\mathrm{e}^{\mathrm{i}kb}}\,. \tag{7}$$

The exact choice for $b$ is not a trivial question. A natural choice can be to consider that $b = d$ because $d$ is the distance between two successive bubbles. Another choice is $b = 0$, which is equivalent to neglecting any correlations in the positions of the scatterers (a gas of point-like scatterers), and interestingly leads to the same result as Foldy's prediction for an infinitely thin layer of bubbly liquid[1]. But it appears that realistic results are obtained when taking for $b$ the distance needed to define a unit cell containing the proper areal fraction of scatterers, which is $b = d/\sqrt{\pi}$. A formal justification is possible for an ordered plane of bubbles, as will be discussed below. With this choice for $b$, it is interesting to note that, providing that $kb \ll 1$, the effective total damping term in equation (5b) has a very clear interpretation. Indeed, it can be written as $\delta + \mathrm{Im}(\tilde{K}a) \simeq 2\pi\delta/(dk)^2 = \delta\lambda^2/(2\pi d^2)$ (where $\lambda$ is the wavelength), which has the form of a *super-radiative* term, due to many bubbles radiating coherently. Thus the radiative damping of a single bubble is enhanced by the factor $\lambda^2/(2\pi d^2)$, which corresponds to the number of bubbles in the area $\lambda^2/2\pi$. As the wavelength we consider here is large, the plane does not need to have a very high concentration of bubbles for $(\lambda/d)^2$ to be large, implying that $F$ is very different from $f$. Another consequence of the interactions between the bubbles in the plane is a shift of the resonance frequency of the system. The maximum of amplitude of $F$ is not reached for the individual resonance of the bubbles but for a higher frequency

$$\omega_{\mathrm{res}} = \frac{\omega_0}{\sqrt{1 - 2\sqrt{\pi}(a/d)}}\,. \tag{8}$$

In Figure 4, the amplitudes of the transmission $T$ predicted by the three different choices for $b$ are plotted in the case of our plane of bubbles. For $b = 0$ the minimum of transmission occurs at the Minnaert resonance of the individual bubbles, which disagrees with the experimental data. For $b = d$, agreement is also poor. On the other hand, $b = d/\sqrt{\pi}$ leads to excellent agreement: both the position and the depth of the dip in transmission (due to the resonance) are precisely predicted. Note that thermal and viscous losses were included in the calculations; neglecting them leads to a lower transmission at the resonance. Using the same parameters, the model also reproduces very precisely the observed sharp jump in the phase of the transmission coefficient at the resonance frequency (Fig. 5).

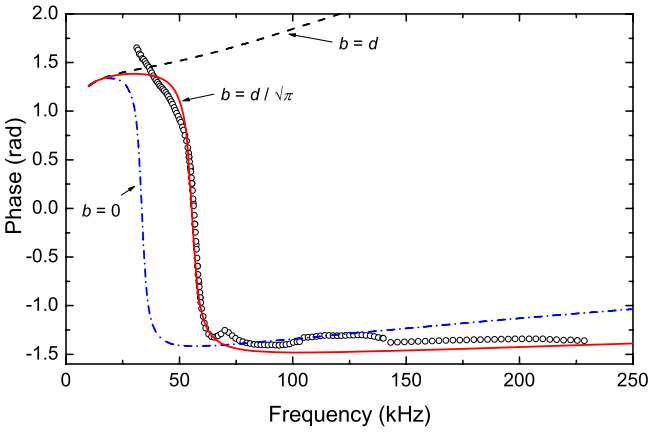


**Fig. 5.** Measured phase of the transmission coefficient through the same sample as in Figure 4 (open circles). A wave propagating through the layer experiences a phase shift of about $+1.5$ rad or $-1.5$ rad for frequencies lower or larger than the resonance frequency, respectively. At the resonance, there is a sharp jump of $\pi$ in the phase. Theoretical results for the three cutoffs considered in the model are also shown by the solid, dashed and dash-dotted lines.

A justification for the choice of the cutoff $b = d/\sqrt{\pi}$ can be found by considering the case of an infinite number of layers of bubbles. Let us assume that identical layers are at $x_n = nd$, with $n \geq 0$. By calculating the total pressure field experienced by each bubble of plane $n$, we can write that the scattering function $F_n$ of layer $n$ is

$$F_n/f = 1 + \tilde{K}F_n + \sum_{j=0}^{n-1} KF_j + \sum_{j=n+1}^{\infty} KF_j\mathrm{e}^{\mathrm{i}2k(j-n)d}. \tag{9}$$

If we look for a solution of the form $F_n = F\mathrm{e}^{\mathrm{i}n(\kappa-k)d}$, two conditions are needed to satisfy equation (9):

$$KF = \mathrm{e}^{\mathrm{i}(\kappa-k)d} - 1, \tag{10a}$$

$$\cos(\kappa d) = \cos(kd) + \mathrm{i}\frac{Kf\sin(kd)}{1 - Kf(\mathrm{e}^{\mathrm{i}kb} - 1)}$$

$$= \cos(kd) - \frac{\frac{2\pi a}{kd^2}\sin(kd)}{\left(\frac{\omega_0}{\omega}\right)^2 - 1 - \mathrm{i}\delta - \mathrm{i}\frac{2\pi a}{kd^2}(\mathrm{e}^{\mathrm{i}kb} - 1)}\,. \tag{10b}$$

Equation (10a) gives the amplitude of the sound wave

[1] See, for example, results in reference [35] when the thickness $h$ tends to 0, for isotropic scatterers.

transmitted through the bubbly medium, and equation (10b) is the dispersion relation[2]. This result is connected to another system that gives additional insight into the problem of determining the cutoff $b$. Indeed, if we consider one bubble in a box, having four side walls that are completely rigid and front and rear walls that are completely free to move, the method of images tells us that this problem is equivalent to an infinite number of ordered planes of bubbles, every bubble of each plane being in phase, and every successive plane being out of phase. Consequently, the modes of the system are found by taking $\kappa d = \pi$ in equation (10b). The point of this analogy is that the bubble in the box is a totally closed system, which means that no radiative losses can occur. Thus, the damping in (10b) must also vanish, leading to the condition on $b$ given by $\cos(kb) = 1 - k^2/(2\pi n)$. This gives a formal justification for our choice of the cutoff $b = d/\sqrt{\pi}$[3]. Note that this demonstration is only valid for perfectly ordered layers but should nonetheless be a good approximation for our partially ordered system (Fig. 4 inset).

Because of this almost ordered state of the sample, it is also appropriate to compare our experimental data with the predictions of multiple scattering theory. MST is known to give accurate results for ordered arrays of scatterers that have simple shapes, such as solid spheres or rods, where the scattering can be calculated exactly. However, for bubbles, an important modification must be made to traditional MST, as there are additional damping mechanisms (the viscous and thermal losses mentioned above) that must be included to give accurate results. To perform these calculations, we used the program MULTEL [44], in which the viscous and thermal losses were incorporated by replacing the sound speed in air by an effective complex sound speed that mimics the effects of these damping mechanisms. The procedure was the following: 1) The Minnaert angular frequency $\omega_0$ and the thermal and viscous damping constant $\delta$ were calculated for the bubbles of our sample (see, for instance, Ref. [26] for detailed equations). 2) The usual dissipation-free resonance frequency of a bubble was written in terms of the velocity of sound in air, $v_\mathrm{a}$, as $\omega_\mathrm{df} = \sqrt{(3\rho_\mathrm{a} v_\mathrm{a}^2)/(a^2\rho_\mathrm{l})}$, where $\rho_\mathrm{a}$ and $\rho_\mathrm{l}$ are the mass density of the air and the liquid, respectively [40]. 3) The effective complex velocity $v_\mathrm{a}^*$ was then determined by the condition that $(3\rho_\mathrm{a} v_\mathrm{a}^{*2})/(a^2\rho_\mathrm{l})$ equals $\omega_0^2 - \mathrm{i}\omega^2\delta$ (*cf.*, Eq. (1)). Because the distributed version of MULTEL only allows constant parameters, we calculated $v_\mathrm{a}^*$ for the central frequency of our bandwidth (100 kHz). However, the frequency dependence was weak enough for this limitation not to yield major errors. This procedure was used to calculate the transmission through a single plane of bubbles arranged in a square array, giving the results shown in Figure 4, which are very close to our approximate theory for this concentration of bubbles.

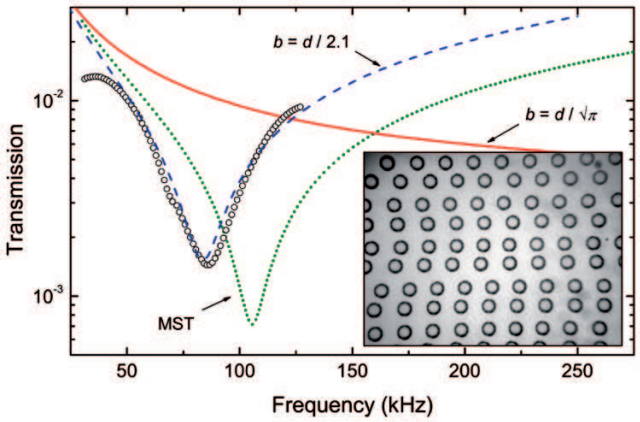


**Fig. 6.** Magnitude of the amplitude transmission coefficient through one layer of 100 $\mu$m radius bubbles separated by 350 $\mu$m (see inset) as a function of frequency. Open circles: experimental data. Solid and dashed lines: model with the cutoffs, $b = d/\sqrt{\pi}$ and $b = d/2.1$ respectively (see text). Dotted line: MST prediction.

Agreement between the experimental data and the theory was satisfactory for all the layers of bubbles we investigated, as long as the concentration of bubbles was low enough. However, equation (8) predicts a qualitative change in the behavior of the plane of bubbles if $d/a < 2\sqrt{\pi} \simeq 3.55$, because $\omega_\mathrm{res}$ becomes imaginary. In order to investigate this prediction, we measured the transmission through a concentrated layer of bubbles for which $d/a = 3.5$ (it corresponds to an area fraction of 26%). As shown in Figure 6, our approximate model (solid black line) does not predict any dip. Experimentaly, the measured transmission through this layer with a higher concentration of bubbles is very similar to the previous one, the difference being that the average transmission is lower and the position of the dip is shifted to higher frequency (86 kHz, whereas the Minnaert resonance of the bubbles is 31 kHz). In fact, our approximate model needs to be extended to take into account the short-range interactions between the bubbles. These interactions have already been described by Strasberg [45] for the simple case of a pair of closely spaced bubbles, using an analogy with the electrostatic interaction between two spherical capacitors. When the two capacitors are close together, the surface charge distribution on each capacitor is no longer spherically symmetric. By analogy, when two bubbles are close together, the oscillation of each bubble is no longer isotropic. This effect results in a small correction when there are only two bubbles, and it has not yet been observed experimentally. In our case, the effect is much larger since many bubbles are involved, and is expected to lead to a significant anisotropy in the bubble oscillations and hence in the radiative acoustic field. Qualitatively, it is easy to see

[2] In the limit of large wavelengths, *i.e.* when $kd$, $\kappa d \ll 1$, $\kappa$ may be interpreted as the effective wave number in the bubbly medium. The choice $b = 0$ for the cutoff leads again to Foldy's formula.

[3] Strictly speaking, the condition brought by the "bubble in the box" argument concerns only the imaginary part of $\tilde{K}$. However, numerical calculations with equation (4) reveal that the real part of $\tilde{K}$ is also well approximated by equation (6) with $b = d/\sqrt{\pi}$, when $kd \ll 1$. Note that in reference [37], Tolstoy and Tolstoy use a mathematical subterfuge to calculate the imaginary part of $\tilde{K}$, in perfect agreement with our result.

that the out-of-plane displacements will be larger than the constrained in-plane displacements. However, a quantitative calculation of the resulting resonance properties becomes very technical and ones loses the benefit of a simple, physically transparent, theory. The multiple scattering approach is then more appropriate. We therefore performed the calculation of the transmission with MULTEL in the case of this higher concentration sample. As shown in Figure 6, the program predicts a dip in transmission, contrary to the approximate theory, but its position and depth do not match the experimental observations. A possible explanation of this discrepancy may come from the imperfect ordering of the sample (see Fig. 6 inset). Figure 6 also shows that, for the approximate theory, it is possible to find a cutoff $b$ that gives a reasonable agreement with the measurements.

It is instructive to examine the physical reasons for the observed *increase* of the resonance frequency. As already mentioned (see Sect. 1), a decrease of the resonance frequency due to the bubble-bubble interactions has been observed for clouds of bubbles [23,26,27]. Indeed, when two bubbles are close to each other, the net effect of their interaction is a decrease in their resonance frequency, because each bubble experiences a pressure field generated by the neighbouring bubble that is in phase with its own pressure field. This can be justified by considering equation (5b) in the special case of two interacting bubbles. Then $\tilde{K}$ reduces to $\mathrm{e}^{\mathrm{i}kd}/d$, where $d$ is the distance between the bubbles, and the resonance occurs for $\omega = \omega_0/\sqrt{1+(a/d)\cos(kd)}$, which is indeed lower than $\omega_0$ for $kd < \pi/2$. However, if the two bubbles are further from each other, the phase between the two pressure fields can change. For example, two bubbles that are $\lambda/2$ apart ($kd = \pi$) will generate fields in anti-phase, leading to an increase of the resonance frequency. If the cloud of bubbles is smaller than half a wavelength, all the contributions are in phase, and the resonance frequency decreases. This situation corresponds to the cases investigated so far in the literature. But for an *infinite* plane of bubbles, both in-phase and out-of-phase contributions exist: bubbles in the first disk of radius $\lambda/4$ contribute to the decrease of the resonance frequency, whereas bubbles in the next ring of thickness $\lambda/2$ tend to increase the resonance frequency. Thus, each successive ring of bubbles brings an opposite contribution. For the particular case of a 2D sample, the contribution of each ring has exactly the same magnitude, because the $1/r$ range of the interaction is exactly compensated by the number of scatterers in each ring. So the net effect is expected to be exactly zero, *i.e.* no frequency shift. Indeed, that is what one obtains with the choice of cutoff $b = 0$. But when the cutoff is not zero, the contribution of the first ring of bubbles is reduced, and the balance of the contributions causes an increase of the resonance frequency, as observed experimentally.

It is interesting to consider the extent to which correlations in the positions of the bubbles may be important for causing the large shifts in the resonances that we observe. It is sometimes assumed that, when the wavelength of the ultrasonic wave is large compared with the distance between the scatterers, the exact positions of the scatterers do not matter [46]. Indeed, our samples were quasi-ordered, and the formal justification of our model is built on an argument for an ordered array. It would also be interesting to check whether the transmission through a totally disordered layer of bubbles is different from a quasi-ordered one. However, with the device we used to inject the bubbles, obtaining a truly disordered layer is challenging, because the radius of the injected bubbles and the distance between them are closely linked (changing the pressure in the syringe or the speed of the capillary affects both $a$ and $d$). Thus, we have not been able to answer this question experimentally, but one can predict on the basis of our model that the appropriate cutoff $b$ in equation (6), which can be taken to be a measure of the correlations, will be different for a random distribution. Indeed for the extreme case of a gas of point-like scatterers, it seems reasonable to take $b = 0$, which would eliminate the shift entirely. For finite-sized scatterers with radius $a$, a more plausible cutoff for a random distribution of scatterers would be $2a$. For bubbles, where $a \ll \lambda$, the result will still be close to the point-scatterer limit and quite different to the ordered case. In general, the exclusion volume around each scatterer will depend on how the samples are made, and larger frequency shifts may be observed because of the resulting position correlations. Thus, it would appear that one should be careful about the neglect of positional correlations in the long-wavelength limit when there are low-frequency resonances, and the measured shift in resonance frequency of an ensemble of scatterers may be quite sensitive to such correlations.

## 4 Conclusions

In this article, we showed that a 2D monodisperse layer of $\sim 100\,\mu$m bubbles efficiently blocks transmitted ultrasound at low frequencies between 30 and 250 kHz. For an area fraction of only 10–20%, the reduction in transmission ranges from $-20$ to $-50$ dB. This is a surprisingly dramatic manifestation of the strong effect of bubbles on ultrasound propagation.

Furthermore, the relatively simple geometry of a single layer of bubbles has enabled us to study the effects of bubble-bubble interactions on their resonances in considerable detail. The transmission through the bubbly layers clearly showed a minimum at a frequency that was much higher than the individual Minnaert frequency of the bubbles, giving a dramatic demonstration of the shift in resonance frequency that can result from the coupling between the bubbles. For a bubble concentration of 10%, the resonance frequency is increased by a factor of 1.7, while for a concentration of 26%, the increase is even larger —a factor of 2.8. To account for this increase quantitatively, we used a self-consistent model, which predicts the resonance of the layer with very good accuracy (for concentration below 15%) and allows the origin of the effect to be understood in a relatively simple way. Similar effects may be expected in other systems with low-frequency resonances, which are a common feature of most metamaterials.

Support from the Natural Sciences and Engineering Research Council of Canada is gratefully acknowledged. We also thank M. Devaud, T. Hocquet and A. Tourin for many fruitful discussions.

## References


1. T. Schwartz, G. Bartal, S. Fishman, M. Segev, Nature **446**, 52 (2007).
2. H. Hu, A. Strybulevych, J.H. Page, S.E. Skipetrov, B.A. van Tiggelen, Nature Phys. **4**, 945 (2008).
3. D.R. Smith, J.B. Pendry, M.C.K. Wiltshire, Science **305**, 788 (2004).
4. M. Minnaert, Philos. Mag. **16**, 235 (1933).
5. S.A. Cheyne, C.T. Stebbings, R.A. Roy, J. Acoust. Soc. Am. **97**, 1621 (1995).
6. M. Kafesaki, R.S. Penciu, E.N. Economou, Phys. Rev. Lett. **84**, 6050 (2000).
7. P.S. Wilson, R.A. Roy, W.M. Carey, J. Acoust. Soc. Am. **117**, 1895 (2005).
8. E.L. Carstensen, L.L. Foldy, J. Acoust. Soc. Am. **19**, 481 (1947).
9. E. Silberman, J. Acoust. Soc. Am. **29**, 925 (1957).
10. R.E. Caflish, M.J. Miksis, G.C. Papanicolaou, T. Ting, J. Fluid Mech. **153**, 259 (1985).
11. M.J. Miksis, L. Ting, J. Acoust. Soc. Am. **86**, 2349 (1989).
12. K.W. Commander, A. Prosperetti, J. Acoust. Soc. Am. **85**, 732 (1989).
13. Z. Ye, L. Ding, J. Acoust. Soc. Am. **98**, 1629 (1995).
14. C. Feuillade, J. Acoust. Soc. Am. **99**, 3412 (1996).
15. F.S. Henyey, J. Acoust. Soc. Am. **105**, 2149 (1999).
16. S.G. Kargl, J. Acoust. Soc. Am. **111**, 168 (2002).
17. A. Strybulevych, V. Leroy, M.G. Scanlon, J.H. Page, Soft Matter **3**, 1388 (2007).
18. P. Sheng, *Introduction to Wave Scattering, Localization, and Mesoscopic Phenomena* (Academic Press, 1995).
19. Z. Ye, J. Acoust. Soc. Am. **102**, 1239 (1997).
20. C. Feuillade, J. Acoust. Soc. Am. **102**, 1242 (1997).
21. F.S. Henyey, J. Acoust. Soc. Am. **111**, 1556 (2002).
22. C. Feuillade, J. Acoust. Soc. Am. **111**, 1552 (2002).
23. P.-Y. Hsiao, M. Devaud, J.-C. Bacri, Eur. Phys. J. E **4**, 5 (2001).
24. R. Manasseh, A. Nikolovska, A. Ooi, S. Yoshida, J. Sound Vibrat. **278**, 807 (2004).
25. E.M.B. Payne, S.J. Illesinghe, A. Ooi, R. Manasseh, J. Acoust. Soc. Am. **118**, 2841 (2005).
26. V. Leroy, M. Devaud, T. Hocquet, J.-C. Bacri, Eur. Phys. J. E **17**, 189 (2005).
27. S.W. Yoon, L.A. Crum, A. Prosperetti, N.Q. Lu, J. Acoust. Soc. Am. **89**, 700 (1991).
28. R.A. Roy, W. Carey, M. Nicholas, J. Schindall, L.A. Crum, J. Acoust. Soc. Am. **92**, 2993 (1992).
29. M. Nicholas, R.A. Roy, L.A. Crum, H. Oguz, A. Prosperetti, J. Acoust. Soc. Am. **95**, 3171 (1994).
30. O. Couture, M. Sprague, E. Cherin, P.N. Burns, F.S. Foster, IEEE UFFC **56**, 536 (2009).
31. V. Leroy, A. Strybulevych, M.G. Scanlon, J.H. Page, J. Acoust. Soc. Am. **123**, 1931 (2008).
32. M. Kafesaki, E. Economou, Phys. Rev. B **60**, 11993 (1999).
33. I. Psarobas, N. Stefanou, A. Modinos, Phys. Rev. B **62**, 278 (2000).
34. Z. Liu, C.T. Chan, P. Sheng, A.L. Goertzen, J.H. Page, Phys. Rev. B **62**, 2446 (2000).
35. Y.C. Angel, C. Aristégui, J. Acoust. Soc. Am. **118**, 72 (2005).
36. D.E. Weston, J. Acoust. Soc. Am. **39**, 316 (1966).
37. I. Tolstoy, A. Tolstoy, J. Acoust. Soc. Am. **87**, 1038 (1990).
38. V. Leroy, M. Devaud, J.-C. Bacri, Am. J. Phys. **70**, 1012 (2002).
39. A. Prosperetti, J. Acoust. Soc. Am. **61**, 17 (1977).
40. T. Leighton, *The Acoustic Bubble* (Academic Press, 1994).
41. P.M. Morse, H. Feshbach, *Methods of Theoretical Physics* (McGraw-Hill, New York, 1953).
42. R.P. Feynman, R.B. Leighton, M. Sands, *The Feynman Lectures on Physics*, Vol. **2** (Addison Wesley, 1971), Chapt. 32.
43. L.L. Foldy, Phys. Rev. **67**, 107 (1945).
44. R. Sainidou, N. Stefanou, I.E. Psarobas, A. Modinos, Comput. Phys. Commun. **166**, 197 (2005).
45. M. Strasberg, J. Acoust. Soc. Am. **25**, 536 (1953).
46. A.A. Ruffa, J. Acoust. Soc. Am. **91**, 1 (1992).